Formation condition of red Ce^{3+} in $Ca_3Sc_2Si_3O_{12}$:Ce^{3+}, N^{3-} as a full-color-emitting light-emitting diode phosphor

Jun Qiao,[1,2] Jiahua Zhang,[1,*] Xia Zhang,[1] Zhendong Hao,[1] Wenyuan Deng,[1] Yongfu Liu,[1] Liangliang Zhang,[1,2] Ligong Zhang,[1] Haifeng Zhao,[1] and Jian Lin[1,2]

[1]*State Key Laboratory of Luminescence and Applications, Changchun Institute of Optics, Fine Mechanics and Physics, Chinese Academy of Sciences, 3888 Eastern South Lake Road, Changchun 130033, China*

[2]*University of Chinese Academy of Sciences, Beijing 100039, China*

**Corresponding author: zhangjh@ciomp.ac.cn*

Received December 18, 2012; revised January 24, 2013; accepted February 11, 2013; posted February 11, 2013 (Doc. ID 181476); published March 12, 2013

In this Letter, we study diffuse reflectance and photoluminescence spectra for O^{2-} fully coordinated green-emitting Ce^{3+} and N^{3-} partially coordinated red Ce^{3+} in $Ca_3Sc_2Si_3O_{12}$(CSS):Ce^{3+}, N^{3-} as a function of CeO_2 and Si_3N_4 contents in the raw material. Our results indicate that the presence of N^{3-} can enhance Ce^{3+} solubility in the form of red centers in CSS. At low Ce^{3+} concentration, green Ce^{3+} forms preferentially while red Ce^{3+} hardly forms even if N^{3-} content in the raw material is sufficient. There exists a threshold concentration of green Ce^{3+}; only beyond that can color tunable luminescence with enriched red emission be achieved. Energy transfer from green Ce^{3+} to red Ce^{3+} is also studied, as only the green Ce^{3+} is excited by blue light. © 2013 Optical Society of America

OCIS codes: 160.2540, 300.6280, 160.4760, 160.4670.

White light-emitting diodes are considered to be promising candidates for a future lighting system [1]; they are commonly fabricated by combining a blue-emitting InGaN chip with $Y_3Al_5O_{12}$:Ce^{3+} (YAG:Ce^{3+}) yellow-emitting garnet phosphor [2]. YAG:Ce^{3+} has a high conversion efficiency, but a less red-emitting component. To resolve this problem, blending YAG:Ce^{3+} with red-emitting phosphors is generally employed [3,4]. The phosphor blend, however, suffers from fluorescence reabsorption that results in loss of luminous efficiency. Hence, full-color-emitting single-phase phosphors are expected. Setlur *et al.* [5] demonstrated that red-emitting Ce^{3+} sites can be created by incorporating N^{3-} into $(Lu,Y,Tb)_3Al_5O_{12}$:Ce^{3+} garnet to replace Al^{3+}-O^{2-} by Si^{4+}-N^{3-}. The red sites are those Ce^{3+} ions that have N^{3-} in their local coordinations. O^{2-} substituted by N^{3-} with a lower electronegativity can result in red shift of the lowest 5d level of Ce^{3+} due to the nephelauxetic effect [5].

Recently, Shimomura *et al.* [6] reported a novel green-emitting silicate garnet phosphor $Ca_3Sc_2Si_3O_{12}$:Ce^{3+} (CSS:Ce^{3+}) in which Ca, Sc, and Si cations are eight-, six-, and four-coordinated in dodecahedron, octahedron, and tetrahedron, respectively [7]. The extended x-ray absorption fine structure analysis indicated that Ce^{3+} ions present at Ca^{2+} sites followed by Ca vacancies are produced for charge compensation [6]. CSS:Ce^{3+} has high emission efficiency and high thermal stability superior to YAG:Ce^{3+}, but it lacks red emissive components to be a full-color-emitting single-phase phosphor. In our previous work [8], we performed N^{3-} incorporation into CSS:Ce^{3+} and achieved red-emitting Ce^{3+} centers (peaked at 610 nm) as the case of YAG [5]. The luminescence spectrum of CSS:Ce^{3+} was then modified to contain an enriched red component so as to generate white light. Ce^{3+} in CSS has a limited solubility around 1.1 mol. % as reported by Shimomura *et al.* [6]. We found that incorporating N^{3-} can enhance additional solubility in the form of red Ce^{3+} centers without reducing the solubility for the original green Ce^{3+}. Furthermore, we also found that the red Ce^{3+} centers hardly form in the case of low concentration of green Ce^{3+}. Obviously, there exists a correlation in the formation of red and the green Ce^{3+} centers. To understand the correlation is therefore of significance for achieving applicable single-phase white phosphor with tunable emission spectra to meet practical demand.

In this Letter, we investigate the formation of green Ce^{3+} and the Ce^{3+} as a function of CeO_2 and Si_3N_4 contents in the raw material. The priority of formation of the two Ce^{3+} centers and emission spectra tuning through energy transfer are reported.

The $Ca_3Sc_2Si_3O_{12}:Ce^{3+}$, N^{3-} (CSS:xCe^{3+}, yN^{3-}) phosphors were synthesized by conventional solid-state reaction. The molar ratio of raw materials was $[CaCO_3]:[CeO_2]:[Sc_2O_3]:[SiO_2]:[Si_3N_4] = (3-x):x:1:(3-0.75y):0.25y$. Two sample series were prepared. For series 1, x was fixed to be 0.06 with y changing from 0 to 1.2. For series 2, y was fixed to be 0.6 with x changing from 0 to 0.15. The mixtures of raw materials were sintered in a tubular furnace at 1350°C for 4 h in reductive atmosphere ($2\%H_2 + 98\%N_2$). The photoluminescence (PL), photoluminescence excitation (PLE), and diffuse reflectance (DR) spectra were measured using a HITACHI F-4500 spectrometer. The fluorescence lifetime was measured by a FL920 Fluorescence Lifetime Spectrometer.

Figure 1(a) shows the DR spectra for CSS:$0.06Ce^{3+}$, yN^{3-} (sample series 1). The absorption band peaking around 450 nm is ascribed to the typical $4f \rightarrow 5d$ transition of Ce^{3+} that substitutes for Ca^{2+} in eight oxygen coordinated dodecahedron in CSS. In the DR spectra for the samples containing N^{3-}, there appears an additional absorption band around 510 nm. This new band has been attributed to the absorption of the Ce^{3+} that has N^{3-} in its local coordination, as described in our previous work [8]. Here we name the Ce^{3+} that has no N^{3-} in its local coordination Ce^{3+}(I), and the Ce^{3+} that has N^{3-} in its local coordination Ce^{3+}(II). In absence of N^{3-}, Shimomura *et al.* have reported that the saturated Ce^{3+}(I) molar concentration available in CSS is 0.011 [6]. The limited solubility of Ce^{3+} in CSS is easily understood

 © 2013 Optical Society of America

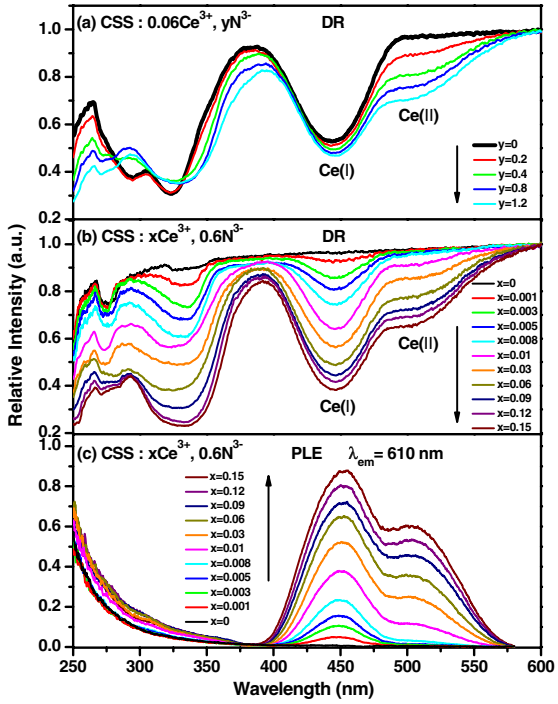

Fig. 1. (Color online) DR spectra for CSS:0.06Ce^{3+}, yN^{3-} (sample series 1) (a), CSS:xCe^{3+}, 0.6N^{3-} (sample series 2) (b), and PLE spectra for sample series 2 (c).

considering the charge difference between Ce^{3+} and Ca^{2+}, which therefore requires generation of Ca vacancies for charge compensation. Obviously, the nominal Ce^{3+} content of 0.06 in the raw material for the present work exceeds the Ce^{3+} condition in material preparation. Hence, the actual Ce^{3+}(I) concentration in the sample CSS:0.06Ce^{3+}, 0N^{3-} (bold curve in Fig. 1) can be deemed to be its saturated concentration of 0.011 in CSS. We can observe in Fig. 1(a) that Ce^{3+}(II) absorption is enhanced considerably when increasing the nominal content (y) of N^{3-} in the raw material; meanwhile, Ce^{3+}(I) absorption only increases slightly. This result indicates that the presence of N^{3-} can promote the total number of Ce^{3+} ions capably incorporated in the CSS host.

The observed remarkable increase of Ce^{3+} solubility in the term of Ce^{3+}(II) type—though not followed by a decrease of the Ce^{3+}(I) type—indicates that the presence of N^{3-} can promote excessive Ce^{3-} in the raw material, which is incorporated into the CSS host to be Ce^{3+}(II). In view of the similar research on nitridation in YAG:Ce^{3+} [5], we deduce that a possible mechanism solution is that Ce^{3+}(II) is formed through a local charge balanced substitution of a Ce^{3+}-N^{3-} pair for a Ca^{2+}-O^{2-} pair in CSS. With regard to the slight increase of Ce^{3+}(I) number with increasing N^{3-}, there are two possible reasons: one is a small delocalized effect of N^{3-} substituting for O^{2-} may on compensating for the positive charge residual of Ce^{3+}, substituting for Ca^{2+} at a long distance; another is N^{3-} with a larger ionic radius substitution for O^{2-} may slightly compensate for the unite cell volume shrinking induced by generation of Ca vacancy in Ce^{3+}(I) formation. What we are interested in is the formation competition between Ce^{3+}(I) and Ce^{3+}(II) as a function of nominal N^{3-} content and Ce^{3+} content in the raw material.

Figure 1(a) demonstrates that the presence of N^{3-} is more beneficial to formation of Ce^{3+}(II) than that of Ce^{3+}(I) in case of excess Ce^{3+} in the raw material. The induced question is how the Ce^{3+} content affects the formation of the two Ce^{3+} centers in case of excess N^{3-} in the raw material. Accordingly, we prepared CSS:xCe^{3+}, 0.6N^{3-} (sample series 2) with fixed nominal N^{3-} content at 0.6 and various nominal Ce^{3+} content x from 0 to 0.15 in the raw material.

Figure 1(b) shows the DR spectra for sample series 2. It is surprisingly observed that the Ce^{3+}(II) absorption band hardly appears as x below 0.008, while Ce^{3+}(I) absorption continuously increases when increasing x. The concentration of incorporated Ce^{3+} ions correlates to their absorptivity in DR spectra. The Ce^{3+}(I) absorptivity (A_1) and Ce^{3+}(II) absorptivity (A_2) are easily obtained from their DR spectra. As the dependence of A_2 on A_1 is plotted, as shown in Fig. 2, we can find that there exists a threshold A_1 for starting growth of A_2. Beyond the threshold, Ce^{3+}(II) begins to form and grows with increasing Ce^{3+}(I) concentration. The threshold A_1 corresponds to nominal Ce^{3+} content close to 0.008. The existence of the threshold indicates that forming Ce^{3+}(I) that substitutes for Ca^{2+} followed by generation of Ca^{2+} vacancy is more easy than Ce^{3+}-N^{3-} substituting for Ca^{2+}-O^{2-} at low Ce^{3+}(I) concentration, even if N^{3-} content in the raw material is more sufficient. Keep this in mind so that the behavior demonstrated in Fig. 2 can be understood. With increasing Ce^{3+}(I) concentration, more generated Ca^{2+} vacancies will shrink the unite cell volume, leading to an increase in the formation energy for Ce^{3+}(I). As Ce^{3+}(I) concentration reaches the threshold, the formation difficulty for Ce^{3+}(I) is raised; meanwhile the formation of Ce^{3+}(II) is stimulated because a large N^{3-} substituting for a small O^{2-} can readily compensate either the positive charge residual or the unite cell volume shrinking induced by Ce^{3+}(I) formation. Consequently, the two centers promote their formation to each other as Ce^{3+}(I) concentration over the threshold.

Figure 3 shows the normalized PL spectra (λ_{ex} = 430 nm) for sample series 2(a)–(c) and series 1 (d). The red spectral components in the PL spectra enhance with increasing x for sample series 2 and with increasing y for sample series 1. Each spectrum can be decomposed into

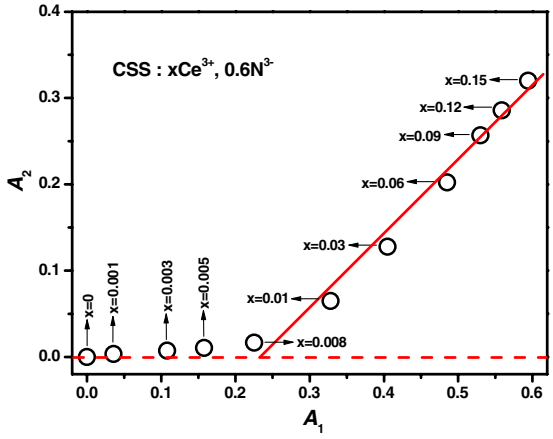

Fig. 2. (Color online) Dependence of A_2 on A_1 in sample series 2.

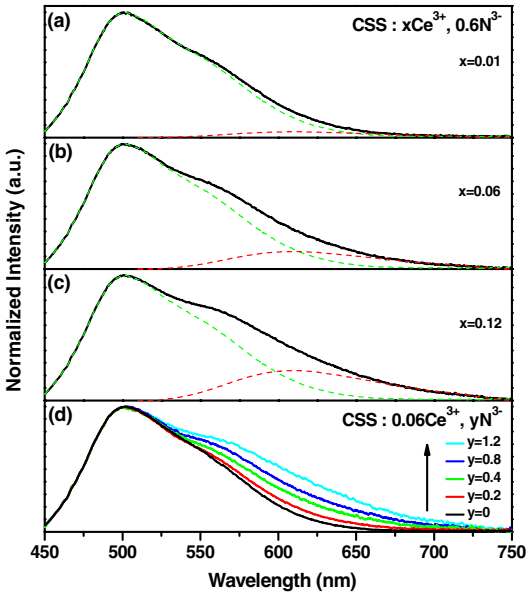

Fig. 3. (Color online) Normalized PL spectra ($\lambda_{ex} = 430$ nm) for sample series 2 (a)–(c) and series 1 (d).

Ce^{3+}(I) and Ce^{3+}(II) emissions. The Ce^{3+}(I) emission spectrum is considered to be one in CSS:Ce^{3+} that exhibits a typical green emission band peaking around 500 nm, as reported in CSS:Ce^{3+} [6]. The Ce^{3+}(II) emission spectrum exhibits a red emission band peaking around 610 nm, as described in our previous work [8]. Their PLE bands are located around 450 and 510 nm, respectively, well consistent with their DR bands, as shown in Fig. 1(c). Considering that the excitation wavelength of 430 nm can only directly excite Ce^{3+}(I) rather than Ce^{3+}(II), the observation of remarkable Ce^{3+}(II) emission therefore indicates occurrence of efficient energy transfer from Ce^{3+}(I) to Ce^{3+}(II). This efficient transfer benefits from a large spectral overlap between the typical green emission band peaking at 500 nm of Ce^{3+}(I) and the PLE band peaking at 510 nm of Ce^{3+}(II). In the PL spectra shown in Fig. 3, the enhancement of the red PL components with increasing x for sample series 2 and with increasing y for sample series 1 reflects the increase in Ce^{3+}(II) number, as demonstrated in their DR spectra. Due to excitation at 430 nm, the excitation of Ce^{3+}(II) is performed completely through Ce^{3+}(I) → Ce^{3+}(II) energy transfer. The emission intensity ratio (I_2/I_1) of Ce^{3+}(II) (I_2) to Ce^{3+}(I) (I_1) is therefore proportional to $\eta/(1-\eta)$, where η is the transfer efficiency, calculated by

$$\eta = 1 - \tau/\tau_0, \tag{1}$$

where τ_0 (62 ns) and τ are average fluorescence lifetimes of Ce^{3+}(I) in absence of Ce^{3+}(II) and in presence of Ce^{3+}(II), respectively. τ is defined as the value of area under the decay curve with normalized initial intensity. Using Eq. (1), the ratio I_2/I_1 should be proportional to $\tau_0/\tau - 1$. As we plot I_2/I_1 versus $\tau_0/\tau - 1$ for sample series 1 and 2 together, these experimental data exhibit a good proportional relationship, as shown in Fig. 4. (I_2/I_1 is normalized to sample series 2 with $x = 0.15$.) This result indicates that the red/green emission intensity ratios fit energy transfer dynamics upon blue light excitation.

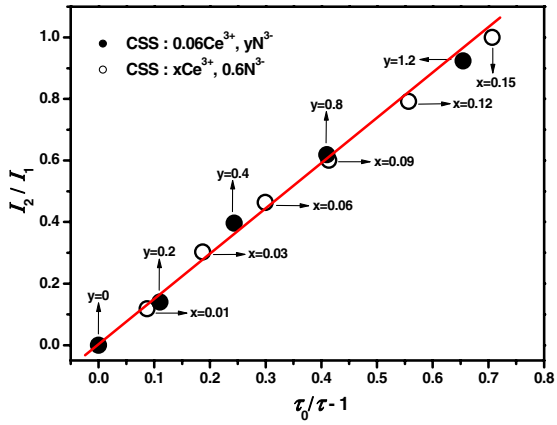

Fig. 4. (Color online) Proportional relationship between I_2/I_1 and $\tau_0/\tau - 1$ for sample series 1 and 2.

In summary, incorporation of N^{3-} in CSS:Ce^{3+} can enhance additional solubility in the form of red Ce^{3+} centers. As CeO_2 content is below 0.008 in the raw material, green Ce^{3+} forms preferentially, while red Ce^{3+} hardly forms, even if Si_3N_4 in the raw material is sufficient. There exists a threshold concentration of green Ce^{3+}; only beyond that can the red Ce^{3+} form. Therefore color tunable luminescence with enriched red emission can be performed through energy transfer from green Ce^{3+} to Ce^{3+}, as only green Ce^{3+} is excited by blue light.

This work was supported by the National Natural Science Foundation of China (grants 10834006, 51172226, 61275055, 10904141, and 10904140).

References

1. E. F. Schubert and J. K. Kim, Science **308**, 1274 (2005).
2. K. Bando, K. Sakano, Y. Noguchi, and Y. Shimizu, J. Light Visual Environ. **22**, 2 (1998).
3. R. J. Xie, N. Hirosaki, T. Suehiro, F. F. Xu, and M. Mitomo, Chem. Mater. **18**, 5578 (2006).
4. J. W. Li, T. Watanabe, N. Sakamoto, H. Wada, T. Setoyama, and M. Yoshimura, Chem. Mater. **20**, 2095 (2008).
5. A. A. Setlur, W. J. Heward, M. E. Hannah, and U. Happek, Chem. Mater. **20**, 6277 (2008).
6. Y. Shimomura, T. Honma, M. Shigeiwa, T. Akai, K. Okamoto, and N. Kijima, J. Electrochem. Soc. **154**, J35 (2007).
7. S. Geller, Z. Kristallogr. **125**, 1 (1967).
8. Y. F. Liu, X. Zhang, Z. D. Hao, X. J. Wang, and J. H. Zhang, J. Mater. Chem. **21**, 6354 (2011).